Supporting Information

Unraveling the anionic oxygen loss and related structural evolution within O3-type Na layered oxide cathode

Min Jia[ab], Yu Qiao*[a], Xiang Li[ab], Kezhu Jiang[c], and Haoshen Zhou*[abc]

[a] *Energy Technology Research Institute, National Institute of Advanced Industrial Science and Technology (AIST), 1-1-1, Umezono, Tsukuba 305-8568, Japan*

[b] *Graduate School of System and Information Engineering, University of Tsukuba 1-1-1, Tennoudai, Tsukuba 305-8573, Japan*

[c] *National Laboratory of Solid State Microstructures & Department of Energy Science and Engineering, Nanjing University, Nanjing 210093, P. R. China*

E-mail: kyou.qiaoyu09206@aist.go.jp; hs.zhou@aist.go.jp & hszhou@nju.edu.cn

Experimental Section

Synthesis of $NaMg_{0.5}Ru_{0.5}O_2$ and $NaMg_{0.67}Ru_{0.33}O_2$ materials:

$NaMg_{0.5}Ru_{0.5}O_2$ materials were synthesized by solid state reaction from stoichiometric amounts of Na_2CO_3, MgO and RuO_2, and amount of Na_2CO_3 was added with 5 wt% excess. The starting stoichiometric mixture was initially ground together and then held at 600 °C for 10 h under argon (Ar) atmosphere. After re-grinding, the powder was heated to 900 °C for another 15 h, again under Ar atmosphere. The resulting dark black powder was reground and carefully checked for impurity phases using x-ray diffraction. And, the corresponding synthesized procedure of $NaMg_{0.67}Ru_{0.33}O_2$ is solid state reaction from stoichiometric amounts of Na_2CO_3, MgO and RuO_2, and amount of Na_2CO_3 was added with 5 wt% excess. The starting stoichiometric mixture was initially ground together and then held at 600 °C for 10 h under air atmosphere. After re-grinding, the powder was heated to 900 °C for another 15 h, again under air atmosphere.

Characterizations:

The structure of $NaMg_{0.5}Ru_{0.5}O_2$ and $NaMg_{0.67}Ru_{0.33}O_2$ materials were identified by powder XRD (Ultima III, Rigaku Corporation) radiation from Cu Kα (λ = 1.5406 Å). The data were collected between diffraction angles (2θ) from 10° to 80° at a scan rate of 2° per min. Rietveld refinements of the XRD pattern obtained by GSAS + EXPGUI suite. The morphologies of the materials were procured by SEM (JSM-7000F). In-situ Raman spectra of the materials were obtained using a homemade mould and JASCO microscope spectrometer (NRS-1000DT).

Electrochemical tests:

2032 coin-type cells were used for electrochemical measurements. The electrodes consisted of active material, acetylene black, and polytetrafluoroethene (PTFE, 12 wt.%) binder with the weight ratio of 80:10:10. 1 M $NaClO_4$ in propylene carbonate (PC) was prepared as the electrolyte.Battery tester system HJ1001 SD8 (Hokuto Denko) were employed for galvanostatic testing.

In-situ Raman observation:

A detailed description of the modified in-situ Raman cell (Hohsen Corp., Osaka, Japan) for the Li-ion battery employed in this study can be found in our previous study.[1] In detail, a thin quartz window (thickness, 0.5 mm) has been fixed on the top of the cell as a sight window. In order to collect shell-isolated nanoparticle-enhanced Raman (SHINER) signal, gold nanoparticles (NPs) approximately 40 nm in diameter with a SiO_2 coating shell (5 nm) were synthesized as in previous reports.[2] The washed and dried Au@SiO_2 NPs were dripped onto the specific cathode surface and vacuum dried before assembly. The cathode was assembled at the bottom of the cell with the active material-face upward. On the top of the cathode, 50-100 μL of electrolyte was homogeneously dropped onto the glassy fiber filter separator (GF/A, Whatman). As a standard two-electrode configuration cell, lithium foil (thickness, 0.4 mm) was assembled at the top as the reference and counter electrode. Note that, a small hole was punched on the center of both the separator and Li foil, through which the laser and Raman signals can fluidly cross. The cell was assembled in an argon-filled glovebox.

The Raman spectra were recorded using a JASCO microscope spectrometer (NRS-1000DT). The excitation light of an air-cooled He−Ne laser at 632.8 nm wavelength was focused on the electrode surface through a 50×long working distance lens (Olympus America Inc.). The confocal slit was adjusted to be 4.0 μm to minimize the band broadening effect due to the contribution of non-confocal signal. The scattered light was collected in a backscattering geometry along the same optical path as the pumping laser. The power of laser beam delivered to the electrode surface was roughly 10% of the maximum 30 mW laser intensity, unless specified, to avoid degradation to the products and/or cathode. The Raman spectrum acquisition time varied from 600~800 s with 2 accumulations. At least 3 different places on the electrode surface at each cathode plate were checked to ensure the Raman spectra were credible and reproducible. The spectral resolution of the Raman spectra in the study was ca.1.0 cm^{-1}.[4]

For the in-situ Raman test, the electrochemical experiments were carried out under the control of a potentiostat (Potentiostat/Galvanostat PGSTAT30, Autolab Co. Ltd., Netherlands) at room temperature. The current and potential outputs from the potentiostat were recorded by a multifunction data acquisition module/amplifier (PGSTAT30 Differential Electrometer, Autolab), which was controlled by General Purpose Electrochemical Software (GPES). Typically, the galvanostatic control was carried out at a current density of 5 mA g^{-1}. Before characterization, the cell was kept

on an open circuit for 10 h. The OCP was approximately 2.7 V in most cases in the study. All of the potentials in this study were referenced to Na/Na^+.

		Na	Mg	Ru
$NaMg_{0.5}Ru_{0.5}O_2$	Conc.	12.2821	6.2880	26.7652
	Stoichiometric ratio	0.534	0.262	0.265
$NaMg_{0.67}Ru_{0.33}O_2$	Conc.	13.2943	9.6582	19.0645
	Stoichiometric ratio	0.578	0.397	0.189

Table S1. Stoichiometry from ICP analysis of the $NaMg_{0.5}Ru_{0.5}O_2$ and $NaMg_{0.67}Ru_{0.33}O_2$ pristine materials.

Refinement results of NMRO		
Phase	$NaMg_{0.5}Ru_{0.5}O_2$	
Space group	R -3 m	
	a (Å)	3.0493(8)
	b (Å)	A
	c (Å)	16.089(4)
Cell parameters	α (°)	90
	B (°)	90
	γ(°)	120
	Cell volume ($Å^3$)	129.55(5)
Agreement factors	Rwp(%)	13.5
	Rp(%)	10.22
	χ^2	3.605

Table S2. Refinement results of $NaMg_{0.5}Ru_{0.5}O_2$

Refinement results of NMRO		
Phase	$NaMg_{0.67}Ru_{0.33}O_2$	
Space group	R -3 m	
	a (Å)	3.04316(5)
	b (Å)	A
	c (Å)	16.1166(4)
Cell parameters	α (°)	90
	B (°)	90
	γ(°)	120
	Cell volume ($Å^3$)	129.256(4)
Agreement factors	Rwp(%)	9.72
	Rp(%)	6.47
	χ2	5.287

Table S3. Refinement results of $NaMg_{0.67}Ru_{0.33}O_2$

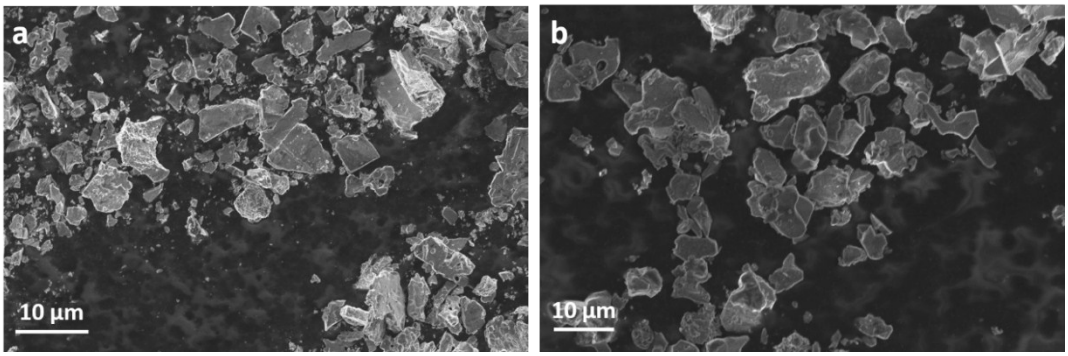

Figure S1. SEM images of $NaMg_{0.5}Ru_{0.5}O_2$ and $NaMg_{0.67}Ru_{0.33}O_2$ pristine material.

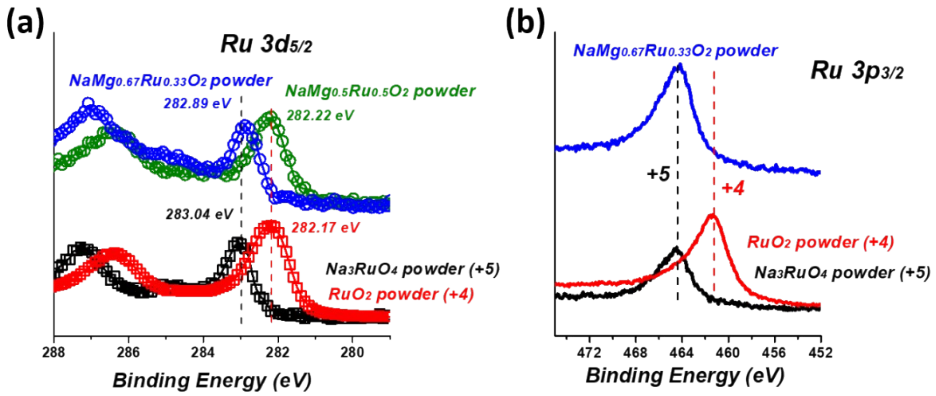

Figure S2. (a) The Ru 3d spectra collected from different compound powder at pristine state. $NaMg_{0.5}Ru_{0.5}O_2$(green line), $NaMg_{0.67}Ru_{0.33}O_2$(blue lines), RuO_2(red lines), Na_3RuO_4(black lines).(b) The Ru 3p spectra collected from different compound powder at pristine state., $NaMg_{0.67}Ru_{0.33}O_2$(blue lines), RuO_2(red lines), Na_3RuO_4(black line)

We used pure original Ru^{4+} model, $\underline{RuO_2}$ and pure original Ru^{5+} prototype model, $\underline{Na_3RuO_4}$ as the corresponding reference. Actually, the binding energy of Ru 3d5/2 for RuO_2 collects at pristine state reveals the core peak at 282.17 eV, and it presents 282.22 eV for $NaMg_{0.5}Ru_{0.5}O_2$. The binding energy of Ru 3d5/2 for Na3RuO4 collects at pristine state reveals the core peak at 283.04 eV, and it presents 282.89 eV for $NaMg_{0.67}Ru_{0.33}O_2$. There is almost no difference between the both.

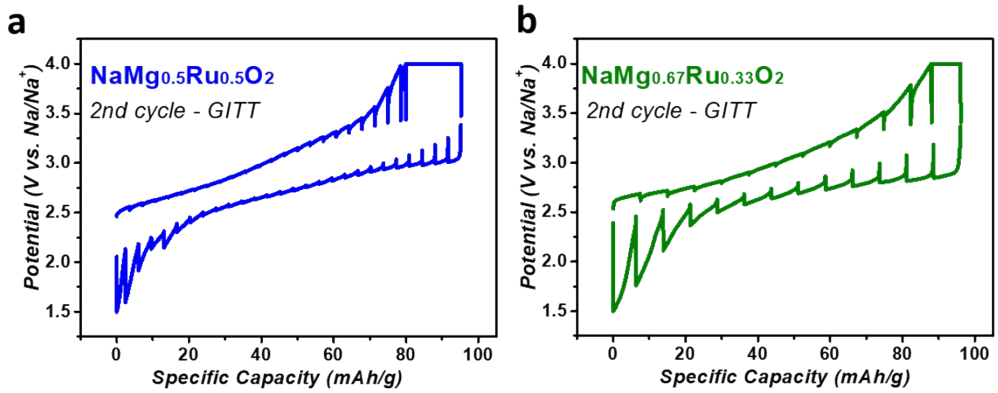

Figure S3. GITT voltage profiles (4 h. C/20 pulse, 20 hr. rest) over the 2nd cycle process for (a)$NaMg_{0.5}Ru_{0.5}O_2$ and (b) $NaMg_{0.67}Ru_{0.33}O_2$ materials.

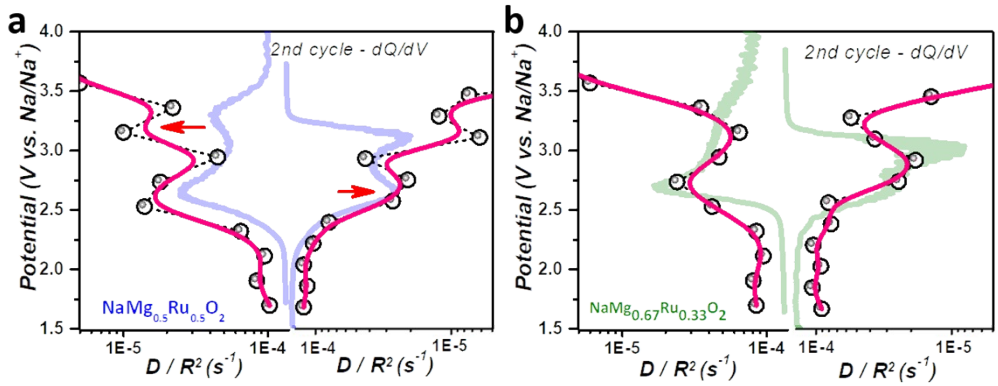

Figure S4. Variation of D/R^2 vs. potential measured with GITT, showing its correlation with the dQ/dV profiles for (a) $NaMg_{0.5}Ru_{0.5}O_2$ and(b) $NaMg_{0.67}Ru_{0.33}O_2$ materials.

Refinement results of NMRO after 50 cycles		
Phase	***$NaMg_{0.5}Ru_{0.5}O_2$ after 50 cycles***	
Space group	***R -3 m***	
	a (Å)	***3.0773(11)***
	b (Å)	***A***
	c (Å)	***16.279(7)***
Cell parameters	***α (°)***	***90***
	B (°)	***90***
	γ(°)	***120***
	Cell volume (Å³)	***133.51(9)***
Agreement factors	***Rwp(%)***	***22.51***
	Rp(%)	***12.46***
	χ2	***19.93***

Table S4. Refinement results of $NaMg_{0.5}Ru_{0.5}O_2$

Refinement results of NMRO after 50 cycles		
Phase	$NaMg_{0.67}Ru_{0.33}O_2$ after 50 cycles	
Space group	R -3 m	
	a (Å)	3.059(4)
	b (Å)	A
	c (Å)	16.048(22)
Cell parameters	α (°)	90
	B (°)	90
	γ(°)	120
	Cell volume ($Å^3$)	130.05(31)
Agreement factors	Rwp(%)	19.51
	Rp(%)	10.83
	χ2	16.86

Table. S5. Refinement results of $NaMg_{0.67}Ru_{0.33}O_2$ after 50 cycles.

Reference:

[1] Y. Qiao, S. Wu, J. Yi, Y. Sun, S. Guo, S. Yang, P. He, H. Zhou, *Angew. Chem. Int. Ed.* **2017**, *56*, 4960.

[2] J. F. Li, Y. F. Huang, Y. Ding, Z. L. Yang, S. B. Li, X. S. Zhou, F. R. Fan, W. Zhang, Z. Y. Zhou, Y. WuDe, B. Ren, Z. L. Wang, Z. Q. Tian, *Nature,* **2010**, *464*, 392